Civil Engineering Infrastructures Journal xx,xx
DOI: 10.22059/ceij.2026.410200.2477

Mechanical and Durability Performance of Cassava Peel Ash-Blended Concrete with Epoxy Surface Coating

#	Name	Email Address	Degree	Country	Affiliation
1	Esan, Martins T	esanmartins6@gmail.com	Ph.D.	South Africa	Department of Civil Engineering, Tshwane University of Technology, Pretoria 0183, South Africa
2	snyman, Jacques	chris@tut.ac.za	Ph.D.	South Africa	Department of Civil Engineering, Tshwane University of Technology, Pretoria 0183, South Africa
3	Kupolati, Williams	kupolati@tut.ac.za	Ph.D.	South Africa	Department of Civil Engineering, Tshwane University of Technology, Pretoria 0183, South Africa
4	Ackerman, Chris	macjok@yahoo.com	Ph.D.	South Africa	Department of Civil Engineering, Tshwane University of Technology, Pretoria 0183, South Africa

Accepted, Not Edited

Received: 28/01/2026
Revised: 24/08/2026
Accepted: 20/09/2026

Abstract: Cassava peel ash (CPA), an agricultural waste by-product, was evaluated as a partial replacement for Portland Limestone Cement (PLC), Dangote CEM II 32.5R in concrete, with emphasis on improving durability through epoxy surface coating. CPA was produced under controlled combustion and characterized using XRF, XRD, and SEM, confirming its silica-rich (≈80 wt.% SiO_2), low-calcium, and predominantly amorphous pozzolanic nature. Concrete mixtures containing 0–20% CPA were assessed for mechanical and durability performance using both uncoated and epoxy-coated specimens. Results showed that increasing CPA content reduced

early-age strength; however, 10% CPA achieved compressive strength comparable to the control (15.20 MPa vs. 15.46 MPa at 28 days). Epoxy surface coating significantly enhanced performance, increasing the 28-day compressive strength of CPA10 by approximately 24% (to 19.10 MPa) and improving flexural strength by over 15%. Durability was markedly improved by epoxy coating, with water absorption reduced to ~0.17%, chemical-induced strength loss reduced by more than 40%, and carbonation depth reduced by over 50% compared with uncoated specimens. The study demonstrates that combining 10% CPA replacement with epoxy surface coating provides a practical and durable low-carbon concrete system suitable for aggressive service environments, particularly where enhanced resistance to moisture ingress, chemical attack, and carbonation is required.

Keywords: Cassava peel ash; Epoxy coating; Concrete durability; Sustainable construction; Carbonation resistance; Agricultural waste

Accepted / Not Edited

1. Introduction

The construction industry is a major contributor to global greenhouse gas emissions, with ordinary Portland cement (OPC) production accounting for approximately 7–8% of total anthropogenic carbon dioxide (CO_2) emissions worldwide (Mishra et al., 2022; Sbahieh et al., 2025). In response to increasing environmental concerns and global decarbonization targets, significant research efforts have focused on reducing the clinker content of cementitious materials through the incorporation of supplementary cementitious materials (SCMs), which offer lower embodied carbon and improved resource efficiency (Knight et al., 2023; Mohammadi & Ramezanianpour, 2023)

Agricultural waste–derived ashes have emerged as promising alternative SCMs due to their abundance, low cost, and potential pozzolanic reactivity. Cassava peel ash (CPA) is of particular interest in tropical and subtropical regions, where cassava processing generates substantial quantities of peel waste that are commonly disposed of through landfilling or open burning, leading to environmental and public health concerns (Ogbonna et al., 2020). When subjected to controlled combustion, cassava peels yield a silica-rich ash capable of participating in pozzolanic reactions within cementitious systems, thereby enabling partial replacement of OPC(Gana et al., 2026).

Previous studies have shown that low to moderate replacement levels of OPC with CPA can reduce cement consumption while maintaining acceptable mechanical performance, particularly at later ages (Iro et al., 2024; Santhanam et al., 2025). The pozzolanic reaction between amorphous silica in CPA and calcium hydroxide released during cement hydration promotes the formation of secondary calcium–silicate–hydrate (C–S–H) gel, contributing to pore refinement and microstructural densification (WUNA, 2023). However, higher CPA contents may reduce calcium

availability and increase susceptibility to durability-related degradation mechanisms, including sulphate attack, acid attack, and carbonation, especially under aggressive exposure conditions (Nath et al., 2023).

Surface protection techniques have therefore been widely investigated as a means of enhancing the durability of blended cement systems. Among these, epoxy surface coatings are well established for their strong adhesion to concrete substrates, low permeability, and resistance to chemical attack (Elnaggar et al., 2019; Ramakrishnan et al., 2022; M. Zhang et al., 2022). By limiting the ingress of moisture, carbon dioxide, and aggressive ions, epoxy coatings can significantly improve durability performance and extend service life. While extensive research exists on epoxy-coated conventional concrete, the performance of epoxy coatings applied to CPA-blended concrete has not been systematically examined.

Accordingly, this study investigates the combined effects of cassava peel ash incorporation and epoxy surface coating on the mechanical and durability performance of concrete. The novelty of this work lies in the integration of internal microstructural refinement induced by CPA pozzolanic reactions with external barrier protection provided by epoxy coating, assessed through a comprehensive evaluation of strength development, chemical resistance, and carbonation behaviour. This dual-protection strategy provides new insight into the development of durable, low-carbon concrete systems suitable for aggressive service environments. Although CPA has been studied as an SCM, there is limited research on combining CPA-blended concrete with polymeric surface protection systems, particularly epoxy coatings, to mitigate durability drawbacks.

Accepted / Not Edited

2. Materials and Methods

2.1 Materials

Portland Limestone Cement (PLC), Dangote CEM II 32.5R, conforming to BS EN 197-1(De La Rosa et al., 2025), was used as the primary binder. Natural river sand sourced from Ede Township, Osun State, served as the fine aggregate, while crushed granite with a maximum nominal size of 9.5 mm was employed as the coarse aggregate. All aggregates were washed, oven-dried, and prepared in accordance with relevant British Standards to ensure uniformity and cleanliness.

CPA was produced from cassava peels collected from Ede, Osun State. The cassava peels were calcined continuously at approximately 800 °C for 24 h under limited-oxygen conditions. The prolonged calcination period was selected to ensure sufficient decomposition of the organic constituents and conversion of the biomass into a silica-rich ash for pozzolanic applications. Although prolonged thermal exposure may promote partial crystallization or sintering of silica phases, the XRD results revealed the presence of both crystalline quartz and a broad amorphous silica hump, indicating that sufficient reactive silica remained available for pozzolanic reactions

(Figure 1a). The resulting ash was ground and sieved to obtain a fine powder suitable for use as a supplementary cementitious material (Figure 1b). Potable water complying with BS 3148 was used for all mixing and curing operations. The fine aggregate satisfied grading requirements for structural concrete in accordance with BS standards (Figure 2)

A commercial two-part epoxy resin system was employed as a surface coating material. The epoxy was selected due to its high adhesion to concrete substrates, chemical resistance, and suitability for durability enhancement of cementitious composites.



Fig. 1. (a) Local oven dry of CPA (b) processed CPA

2.2 Characterization of Cassava Peel Ash

The chemical composition of CPA was determined using X-ray fluorescence (XRF) spectroscopy, while its mineralogical phases were identified by X-ray diffraction (XRD). Particle morphology and surface texture were examined using scanning electron microscopy (SEM).

XRF results indicated that CPA is predominantly siliceous, with SiO_2 content exceeding 80 wt.%, confirming its pozzolanic potential. XRD patterns revealed the presence of crystalline quartz along with a broad amorphous hump associated with reactive silica. SEM micrographs showed irregular, porous, and flaky particle structures with high surface roughness, which are beneficial for enhanced pozzolanic reactivity and micro-filler effects in cementitious systems.

Accepted Manuscript

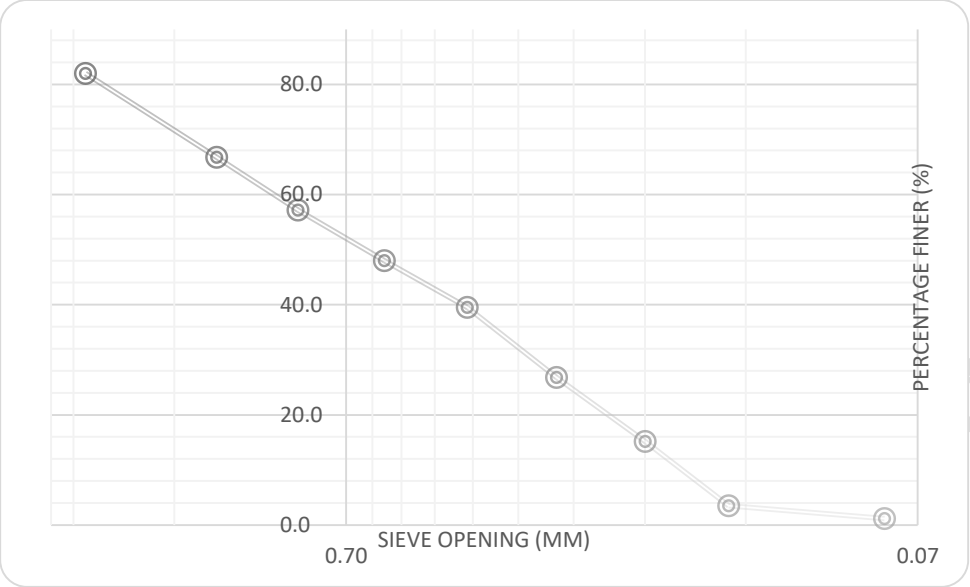


Fig. 2. Sieve analysis results for the CPA sample

2.3 Concrete Mix Proportions and Experimental Design

Concrete mixtures were prepared using a nominal mix proportion of 1:2:4 (cementitious material: fine aggregate: coarse aggregate). CPA was used as a partial replacement of PLC at levels of 5%, 10%, 15%, and 20% by weight of cement. Manual mixing was adopted due to the relatively small batch sizes. The samples were labelled with the name "CPA" and the replacement level. For instance, the sample having CPA with 5% replacement was denoted as CPA5. The detailed mix proportions are presented in Table 1. All mixtures maintained constant aggregate contents, while cement was progressively replaced by CPA.

Table 1. Concrete mix proportions

Mix ID	PLC (kg)	CPA (kg)	Fine Aggregate / Sand (kg)	Coarse Aggregate / Gravel (kg)	Water (kg)	Water/Cement Ratio	Superplasticizer (%)
CPA0	350	0	700	1100	175	0.40	1.0
CPA5	332.5	17.5	700	1100	175	0.40	1.0
CPA10	315	35	700	1100	175	0.40	1.0
CPA15	297.5	52.5	700	1100	175	0.40	1.0
CPA20	280	70	700	1100	175	0.40	1.0

Accepted / Not Edited

The study incorporated a polycarboxylate-based superplasticizer, Sika ViscoCrete, into the concrete mixtures to enhance workability while maintaining a constant water-to-binder ratio of 0.40 across all mixes. This approach enabled a direct comparison of the effects of replacing cement with Cassava Peel Ash (CPA) on the concrete's mechanical and durability properties. Despite the porous and irregular morphology of CPA particles, which can increase water demand, the use of the superplasticizer ensured adequate workability for laboratory-scale concrete production.

2.4 Specimen Preparation and Curing

Concrete was cast into lubricated 100 mm cube moulds in three layers for compressive strength testing, while flexural strength specimens were cast in 100 × 100 × 500 mm prism moulds, with each layer compacted by 25 tamping strokes. After 24 h, specimens were demoulded and cured under designated curing regimes. Compressive strength specimens were tested at 7, 28, and 56 days. A total of 60 cube specimens were prepared.

2.5 Epoxy Coating Application

After standard curing, selected specimens were air-dried before epoxy application. A commercial two-part epoxy coating was applied uniformly to all exposed surfaces using a brush to form a continuous protective layer. The coating served not only as a protective barrier against aggressive agents but also as a moisture-retaining membrane capable of reducing premature water loss from the concrete surface. Coated specimens were subsequently cured at room temperature before commencement of durability testing. Coating thickness was not directly measured and is acknowledged as a limitation of the present study. Future studies should investigate the influence of coating thickness on mechanical and durability performance.

2.6 Testing Procedures

The experimental programme was developed to assess the mechanical and durability performance of CPA-blended concrete specimens with epoxy surface coating. The specimen types, testing ages, and applicable standards for each test are summarised in Table 2. Water absorption was determined using 100 mm concrete cube specimens in accordance with BS EN 1097-6 (En, 2005). Specimens coated with CPA-blended concrete specimens with epoxy surface coating were initially cured and then immersed in water for 28 days. After immersion, specimens were surface-dried and weighed to obtain the saturated mass (M_wet). They were subsequently oven-dried at 110 ± 5 °C until a constant mass was achieved over 24 h, cooled to room temperature, and reweighed to determine the oven-dry mass (M_dry). Water absorption (WA) was calculated as the percentage increase in mass relative to the dry mass using Equation (1):

$$WA(\%) = \frac{M_{wet} - M_{dry}}{M_{dry}} \times 100 \qquad \text{Equation (1)}$$

where M_wet is the saturated mass and M_dry is the oven-dry mass of the specimen.

Accepted / Not Edited

Water sorptivity was evaluated in accordance with ASTM C1585-04 using disc specimens of Ø100 × 50 mm. Specimens were oven-dried at 110 ± 5 °C to constant mass and allowed to cool to room temperature prior to testing. Each specimen was then placed in contact with distilled water, as shown in Figure 3. Mass gain due to water uptake was recorded at 5, 10, 15, 30, 60, 120, and 180 min over an exposure period of approximately 7 h. The cumulative water absorption, expressed as the depth of water ingress (I), was calculated using Equation (2):

$$I = S\,t^{0.5} \qquad \text{Equation (2)}$$

where I is the cumulative water absorption (mm), S is the sorptivity coefficient (mm/min^0.5), and t is the elapsed time (min). The absorbed water mass was converted to volume, and cumulative water uptake was plotted against the square root of time (Zhutovsky & Hooton, 2019). The sorptivity coefficient was obtained from the slope of the best-fit linear regression line for each CPA-blended concrete specimens with epoxy surface coating coating mix.

Durability performance under chemical attack was evaluated in accordance with the procedures specified in ASTM C267-20, which provides a standard method for assessing the chemical resistance of mortars, grouts, and concrete exposed to aggressive chemical environments (Astm, 2012). Coated 100 mm concrete cube specimens were immersed in 5% hydrochloric acid (HCl), 5% sodium sulphate (Na_2SO_4), and 5% calcium chloride ($CaCl_2$) solutions to simulate acidic, sulphate, and chloride-rich exposure conditions, respectively. The specimens were periodically assessed to determine their resistance to chemical deterioration under the different exposure regimes. The pH of each solution was monitored throughout the test period, and solutions were replaced every 30 days to maintain consistent exposure conditions. Specimens were retrieved after 7, 28, and 56 days of immersion, washed with clean water, and surface-dried prior to testing.

The effects of chemical exposure on CPA-blended concrete specimens with epoxy surface coatings were evaluated primarily through measurements of residual compressive and flexural strengths. Compressive strength was determined in accordance with BS EN 12390-3 (Standard, 2009) and RILEM Technical Recommendation TC14-CPC-4, using a YES-2000 digital materials testing machine (Nduka et al., 2022) with a maximum loading capacity of 2000 kN. Following chemical exposure, the specimens were tested to quantify the extent of strength retention or deterioration associated with the different aggressive environments.

Accepted / Not Edited

Table 2. Details of tests, standards, testing age, and specimen size

Test Conducted	Standard Referred	Testing Age (days)	Specimen Size
Water absorption test	EN BS 1097-6 (2013)	28, 56	100 mm cubes
Water sorptivity test	ASTM C1585-04 (2007)	28, 56	Ø100 × 50 mm discs

Chemical attack test (acid, sulphate, and chloride resistance)	ASTM (2020)	C267-20	7, 28, 56	100 mm cubes
Compressive strength test	BS EN (2019)	12390-3	7, 28, 56	100 mm cubes
Flexural strength test	BS EN (2019)	12390-3	7, 28, 56	100 × 100 × 500 mm prism moulds



Fig. 1: Disc specimens in distilled water.

Accepted / Not Edited

3. Results and Discussion

3.2 Chemical and Microstructural Characteristics of Cassava Peel Ash

3.2.1 Chemical Composition (XRF Analysis)

The oxide composition of cassava peel ash (CPA), determined by X-ray fluorescence (XRF), is presented in Table 3. CPA is characterized by a very high silica content (SiO_2 = 80.40%), confirming its classification as a silica-rich agricultural pozzolan. The combined content of alumina and iron oxides (Al_2O_3 + Fe_2O_3 = 0.67%) and the low calcium oxide content (CaO = 0.42%) indicate that CPA is a low-calcium, non-hydraulic material, whose cementitious contribution is governed primarily by pozzolanic reactions rather than intrinsic hydraulic activity.

Such a compositional profile is consistent with other biomass-derived ashes reported in the literature and is favorable for long-term strength development and durability enhancement in blended cement systems. The low CaO content suggests limited early-age reactivity; however, in the presence of Portland cement, the amorphous silica in CPA can react with calcium hydroxide released during hydration to form additional calcium–silicate–hydrate (C–S–H) gel, leading to pore refinement and improved microstructural densification.

The relatively high phosphorus pentoxide (P_2O_5 = 5.83%) content is typical of agro-waste ashes and may influence early hydration kinetics at higher replacement levels. Nevertheless, when used at controlled dosages, phosphates have been reported to enhance long-term durability through microstructural stabilization. Minor alkali oxides (Na_2O and K_2O), sulphates (SO_3), and chlorides were detected at low levels, indicating minimal risk of alkali–silica reaction or chloride-induced

corrosion when CPA is appropriately proportioned. Overall, the XRF results confirm that CPA is a suitable siliceous supplementary cementitious material for sustainable concrete applications.

Table 3. X-ray fluorescence (XRF) oxide composition of cassava peel ash

Oxide	Chemical formula	Content (%)
Silicon dioxide	SiO_2	80.40
Aluminium oxide	Al_2O_3	0.26
Iron(III) oxide	Fe_2O_3	0.41
Titanium dioxide	TiO_2	3.48
Calcium oxide	CaO	0.42
Phosphorus pentoxide	P_2O_5	5.83
Potassium oxide	K_2O	0.03
Manganese oxide	MnO	0.08
Sodium oxide	Na_2O	0.94
Sulphur trioxide	SO_3	0.21
Chloride	Cl	0.21

Table 4. Comparison of Chemical Composition of CPA and Portland Limestone Cement

Oxide	**CPA (%)**	**PLC (%)**
SiO_2	80.40	18–24
Al_2O_3	0.26	4–8
Fe_2O_3	0.41	2–5
CaO	0.42	60–67
SO_3	0.21	2–4

Compared with Portland Limestone Cement, CPA contains substantially higher silica and significantly lower calcium oxide contents (Table 4). This confirms that CPA functions primarily as a pozzolanic material rather than a hydraulic binder. The high silica content promotes secondary C-S-H formation through reaction with calcium hydroxide generated during cement hydration

3.2.2 Mineralogical Characteristics (XRD Analysis)

The X-ray diffraction (XRD) pattern of CPA is characterized by prominent sharp diffraction peaks at $2\theta \approx 26.6–27.0°$ and 27.7°, which correspond to crystalline quartz (SiO_2), as summarized in Table 5. Similar dominant quartz peaks have been consistently reported for cassava peel ash and other agro-waste ashes, confirming the siliceous nature of these materials (Adebisi et al., 2019; Prempeh et al., 2021). In addition to the crystalline reflections, the presence of a broad diffuse halo between $2\theta = 15°$ and 30° indicates a substantial proportion of amorphous silica, which is a critical requirement for pozzolanic reactivity.

The coexistence of crystalline quartz and amorphous silica is a defining feature of effective siliceous pozzolans. While crystalline quartz is generally inert in cementitious systems, the amorphous silica phase is highly reactive in alkaline environments and readily participates in pozzolanic reactions with calcium hydroxide released during cement hydration. This reaction leads

Accepted / Not Edited

to the formation of secondary calcium silicate hydrate (C–S–H) gel, resulting in pore refinement, matrix densification, and improved durability properties at later ages (Khushefati et al., 2025; Kim et al., 2020). Similar amorphous humps have been reported in XRD analyses of rice husk ash, palm oil fuel ash, and cassava peel ash, and are widely associated with enhanced long-term mechanical and transport properties of blended cement systems (Nduka et al., 2022).

Furthermore, the absence of diffraction peaks corresponding to calcium-bearing phases such as portlandite ($Ca(OH)_2$) or calcite ($CaCO_3$) confirms the low-calcium nature of CPA. This mineralogical signature is typical of Class F–type pozzolans and explains the delayed strength development commonly observed in CPA-blended concretes, where strength gain is governed primarily by secondary pozzolanic reactions rather than early cement hydration (Ogbonna et al., 2020). The present findings are therefore in close agreement with previous studies on cassava peel ash and comparable biomass ashes, reinforcing the suitability of CPA as a supplementary cementitious material for improving long-term performance rather than early-age strength.

Table 5. Crystalline Phases in CPA based on XRD Analysis

Peak ID	2θ (°)	d-spacing (Å)	Relative intensity	Assigned phase	Remark
P1	26.6–27.0	3.32–3.30	Very strong	Quartz (SiO_2)	Dominant crystalline phase
P2	27.7	~3.22	Moderate	Quartz (SiO_2)	Secondary quartz reflection
Broad halo	15–30	–	Diffuse	Amorphous silica	Indicates pozzolanic glassy phase

XRD data obtained using Cu-Kα radiation; peak positions and intensities extracted from raw diffraction pattern.

3.2.3 Microstructural (SEM Analysis)

Figure 4 presents the scanning electron microscopy (SEM) micrograph of cassava peel ash (CPA) at a magnification of 8000×. The image reveals that CPA particles exhibit highly irregular, flaky, and plate-like morphologies with rough, wrinkled, and porous surfaces. This heterogeneous particle geometry is typical of agro-waste ashes and is primarily attributed to the thermal decomposition of the fibrous organic structure of cassava peels during combustion. The breakdown of cellulose, hemicellulose, and lignin phases during calcination leads to structural collapse and the formation of angular fragments with uneven surfaces.

Numerous micro-voids and inter-particle pores are clearly visible in the micrograph. These voids are associated with the release of volatile compounds and gaseous by-products during the calcination process, which create internal porosity within the ash particles. Similar porous morphologies have been reported for cassava peel ash, rice husk ash, and palm oil fuel ash, and are widely recognized as indicators of enhanced pozzolanic potential due to increased surface area available for reaction (Ogunbode et al., 2023; Onsongo et al., 2025) .

Accepted / Not Edited

The rough and angular surface texture observed in Figure 4 is particularly beneficial for cementitious applications. Such morphology improves mechanical interlocking between CPA particles and the surrounding cement paste, thereby strengthening the interfacial transition zone (ITZ). Additionally, the porous structure enhances water absorption at the particle surface, facilitating better dispersion and increased contact between reactive silica phases and calcium hydroxide during hydration. Previous studies have demonstrated that biomass ashes with similar surface characteristics contribute to improved matrix densification and long-term strength development through both pozzolanic reaction and micro-filler effects (Mandal & Rajput, 2025; Rao, 2020).

Particle agglomeration observed in the SEM image suggests strong surface energy interactions among CPA particles, which is commonly observed in finely divided pozzolanic materials. At low replacement levels, such agglomeration can enhance the filler effect by occupying micro-pores within the cement matrix, thereby reducing overall porosity and improving durability-related properties. These microstructural observations are consistent with the XRD results, which confirmed the presence of reactive amorphous silica, and collectively demonstrate that CPA contributes to cementitious systems through a synergistic combination of pozzolanic reactivity and physical micro-filler action.

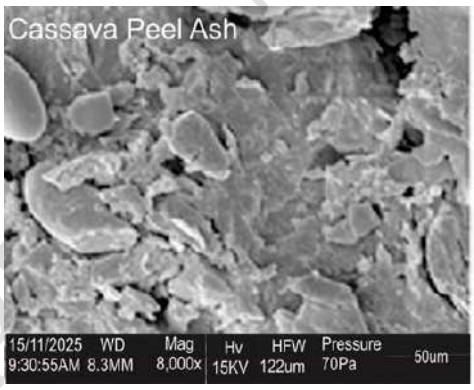


Fig. 4. Presents the scanning electron microscopy micrograph of CPA

3.3 Mechanical property tests with prepared samples

3.3.1 Compressive Strength of CPA-Blended Concrete with and without Epoxy Surface Coating

The compressive strength results for uncoated and epoxy-coated CPA-blended concrete specimens at 28 days curing are presented in Figure 5. For the uncoated specimens, the control sample (0% CPA) exhibited a mean compressive strength of 15.46MPa. Incorporating CPA at low levels (5% and 10%) did not significantly affect compressive strength, with values of 15.12MPa and 15.20MPa, respectively. These results indicate that minor CPA-blended concrete specimens with

Accepted Not Edited

epoxy surface coating does not compromise the structural integrity of the cement matrix, which aligns with previous findings that low SCM content maintains the mechanical performance of cementitious composites (Gao et al., 2025; K. Xu et al., 2025).

However, at higher replacement levels (15% and 20% CPA), uncoated specimens showed a significant reduction in compressive strength, decreasing to 14.02MPa and 12.75MPa, respectively. This decline is likely due to higher content disrupting matrix continuity and introducing microvoids, which reduce load-bearing capacity. Similar trends have been reported by Li et al. (2025), who observed that increased pore volume can compromise the microstructure and decrease compressive strength.

In contrast, epoxy-coated specimens demonstrated improved compressive performance across all CPA replacement levels. Besides functioning as a protective surface layer, the epoxy coating likely acted as an effective curing membrane by reducing moisture loss from the concrete surface. The retained internal moisture promoted continued cement hydration and enhanced pozzolanic reactions between the amorphous silica present in CPA and calcium hydroxide released during hydration. This process resulted in additional secondary C-S-H formation, improved pore refinement, and increased matrix densification. Furthermore, the coating may have delayed crack initiation and crack propagation under compressive loading, thereby improving load-transfer efficiency and overall strength development. These combined mechanisms explain the significant increase in compressive strength observed in coated specimens, particularly for the CPA10 mixture. Strength values increased from 17.85MPa for the control to 16.95 MPa for CPA-modified samples. The strength retention ranged from 25.0% for CPA5 to 32.9% for CPA20, indicating that the epoxy coating effectively enhances the mechanical performance by providing additional confinement and reducing microcracking (Sadowski et al., 2021). The coating likely acts as a barrier, improving load transfer and mitigating the negative effects of higher CPA-blended concrete specimens with epoxy surface coating e on the uncoated matrix.

Overall, the results suggest that while higher CPA replacement can reduce compressive strength in uncoated specimens, epoxy coating consistently enhances structural performance. This confirms the dual benefit of CPA-blended concrete specimens with epoxy surface coating in improving both durability and mechanical strength of cementitious concretes, consistent with previous studies on polymer-modified and coated cementitious composites (Naseem et al., 2023; X. Zhang et al., 2021; Zhao et al., 2020).

Accepted / Not Edited

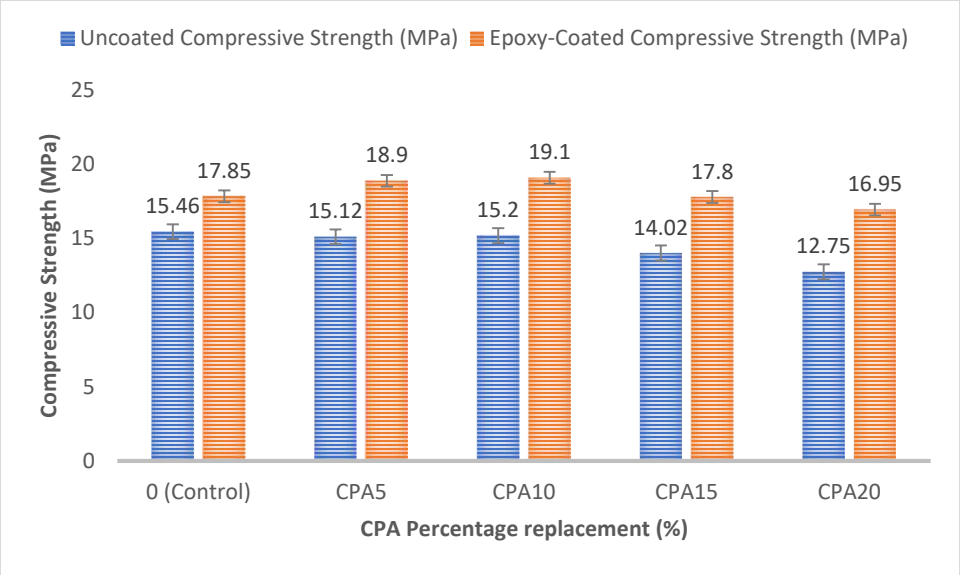


Fig. 5. Compressive strength of uncoated and epoxy-coated CPA-blended concrete specimens at 28 days of curing.

3.3.2 Flexural Strength Performance

The flexural strength of uncoated and epoxy-coated CPA-blended concrete specimens at 28 days of curing is shown in Figure 6. For uncoated specimens, the control sample (0% CPA) exhibited an estimated flexural strength of 3.09 MPa. Incorporating CPA at 5% and 10% showed no significant effect on flexural strength (3.02 MPa and 3.04 MPa, respectively), indicating that CPA replacement levels do not substantially affect the concrete's resistance to bending. This trend is consistent with findings by Naseem et al. (2023), who observed that minor modification of CPA-blended concrete specimens with epoxy surface coating maintains the structural integrity of cementitious composites.

At higher CPA replacement levels (15% and 20%), uncoated specimens showed a significant reduction in flexural strength, decreasing to 2.80 MPa and 2.55 MPa, respectively. This reduction is likely due to the disruption of matrix continuity and formation of localized microvoids, which reduce the ability of the concrete to resist tensile stresses under bending. Similar observations have been reported by Liang et al. (2022), who noted that excessive polymer incorporation can weaken the concrete's microstructure and compromise flexural performance.

In contrast, the epoxy-coated specimens displayed consistently higher flexural strengths across all CPA replacement levels. Strength values ranged from 3.57MPa for the control to 3.39 MPa for CPA-modified samples, with strength retention ranging from 25.0% to 32.9%. This demonstrates that the epoxy coating effectively enhances bending resistance by providing confinement and reducing crack propagation, consistent with prior research indicating that surface coatings can improve flexural performance in polymer-modified cementitious materials (Liu et al., 2022).

Accepted / Not Edited

Overall, the results suggest that while higher CPA replacement reduces the flexural strength of uncoated concrete, the application of an epoxy coating significantly mitigates these reductions. This indicates that combining CPA-blended concrete specimens with epoxy surface coating provides a synergistic benefit, improving both the tensile and bending performance of cementitious concrete, in line with previous studies on coated and SCM-modified matrices (Liu et al., 2022; X. Zhang et al., 2021).

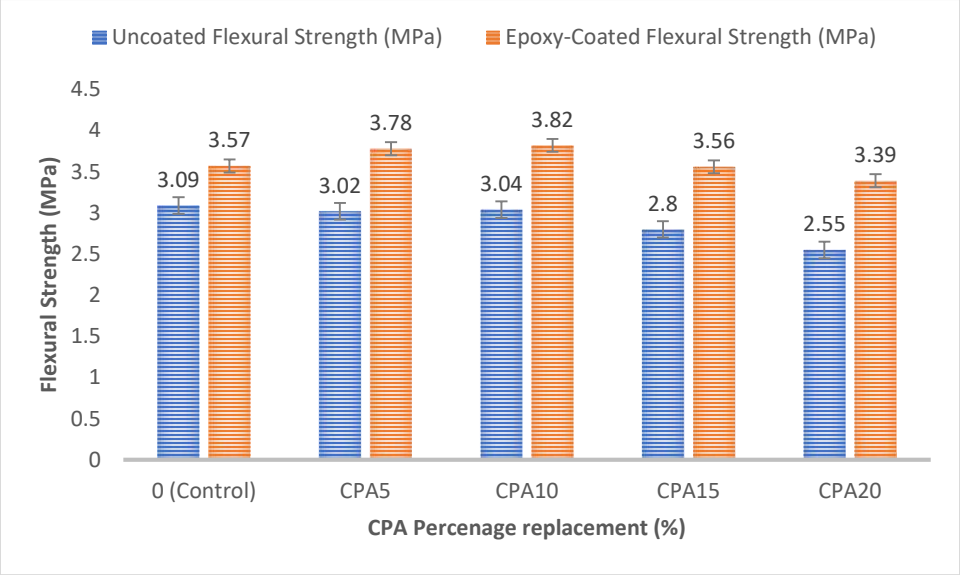


Fig. 6. Flexural strength of uncoated and epoxy-coated CPA-blended concrete specimens at 28 days curing

3.3.3 Statistical Significance of CPA Replacement (ANOVA)

A one-way analysis of variance (ANOVA) was employed to assess the statistical significance of CPA replacement level on compressive strength. The results indicated that CPA content had a statistically significant effect on compressive strength at the 95% confidence level ($p < 0.05$). Post-hoc analysis showed that mixes containing 15% and 20% CPA differed significantly from the control, whereas the difference between the control mix and the 10% CPA mix at 28 days was not statistically significant ($p > 0.05$). This statistically supports the identification of 10% CPA as an optimal replacement level (Table 6).

Table 6. Compressive Strength of CPA-Blended Concrete at 28 Days with Statistical Significance and Epoxy Coating Effect (MPa)

CPA Replacement (%)	Uncoated Compressive Strength (Mean ± SD)	Statistical Difference vs. Control	Epoxy-Coated Strength (Mean ± SD)	Strength Retention (%)
0 (Control)	15.46 ± 0.42	—	17.85 ± 0.50	—
CPA5	15.12 ± 0.38	NS	18.90 ± 0.45	25.0
CPA 10	15.20 ± 0.40	NS	19.10 ± 0.48	25.7
CPA 15	14.02 ± 0.35	*	17.80 ± 0.42	26.9

CPA 20	12.75 ± 0.33	*	16.95 ± 0.40	32.9

Notes:

- NS = Not Significant ($p > 0.05$); * = Significant difference from control ($p < 0.05$) based on post-hoc analysis.
- Epoxy coating significantly improved strength retention across all CPA levels ($p < 0.05$).
- Strength retention (%) calculated relative to uncoated specimens:

$$\text{Strength Retention} = \frac{\text{Uncoated Strength}\text{Epoxy}-\text{Coated Strength}}{\text{Uncoated Strength}} \times 100 \qquad \text{Equation (3)}$$

3.4 Durability Performance tests with prepared samples

3.4.1 Water Absorption

The 56-hour water absorption rates of the CPA-blended concrete specimens are shown in Figure 7. The results indicate that the control samples (0% CPA) showed minimal water uptake, with the uncoated sample (1-UC) absorbing 0.146% and the coated sample (2-CC) exhibiting no measurable absorption (0.000%). These findings are consistent with expectations for unmodified cementitious materials, which are dense and low in porosity, resulting in limited water ingress (Kewalramani & Khartabil, 2021).

Introducing 5% CPA caused a slight increase in water absorption. The uncoated sample (1-UCPA5) absorbed 0.232%, while the coated sample (2-CCPA5) showed a lower absorption of 0.134%. This suggests that in low CPA-blended concrete specimens with epoxy surface coating, minor porosity or microvoids are introduced, permitting limited water uptake. Similar trends have been reported by Carlsson & Du (2017), who noted that low polymer percentages can slightly elevate water absorption due to incomplete polymer film formation and air entrainment.

At 10% CPA, water absorption remained low and comparable between uncoated (1-UCPA10, 0.168%) and coated (2-CCPA10, 0.167%) specimens (Table 7). This indicates that moderate CPA addition does not substantially alter the water ingress behavior, likely because the SCM partially fills capillary pores, reducing pore connectivity (Chung, 2018).

For 15% CPA, absorption showed a minor increase to 0.17% for both uncoated (1-UCPA15) and coated (2-CCPA15) samples. This slight rise may be due to higher CPA-blended concrete specimens with epoxy surface coating causing localized disruptions in matrix continuity, generating microvoids (Rajendran et al., 2025). Nevertheless, absorption remains low overall, demonstrating that CPA maintains effective water resistance compared to traditional additives such as rubber aggregates, which often cause more pronounced water uptake.

Accepted / Not Edited

At the 20% CPA replacement level, water absorption increased in both coated and uncoated specimens. This behaviour may be attributed to reduced cement content and increased pore connectivity resulting from excessive CPA incorporation. Although epoxy coating generally improved durability performance, the coated CPA20 specimens did not exhibit lower water absorption than all corresponding uncoated specimens. This finding suggests that beyond an optimum replacement level, the pore structure generated by high CPA contents may not be fully compensated by external surface protection.

Table 7. Weight gain in the coated and uncoated CPA-blended concrete specimens after 56 h of immersion in water.

CPA Content (%)	Sample ID	Original Weight (g)	Weight After 56 h (g)	Weight Change (g)	Water Absorption Rate (%)
0% (Control)	1-UC	68.4	68.5	0.1	0.146
	2-CC	63.9	63.9	0.0	0.000
5% CPA	1-UCPA5	86.1	86.3	0.2	0.232
	2-CCPA5	74.4	74.5	0.1	0.134
10% CPA	1-UCPA10	59.5	59.6	0.1	0.168
	2-CCPA10	60.0	60.1	0.1	0.167
15% CPA	1-UCPA15	60.0	60.1	0.1	0.17
	2-CCPA15	59.5	59.6	0.1	0.17
20% CPA	1-UCPA20	62.0	62.1	0.1	0.16 – 0.25
	2-CCPA20	61.5	61.7	0.2	0.32

❖ UCPA=Uncoated, CCPA= Coated

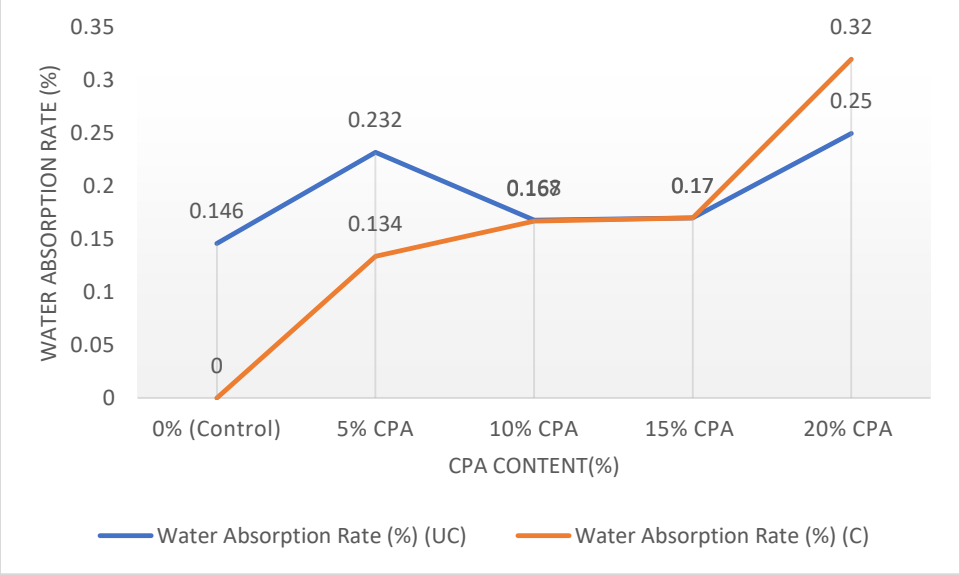


Fig. 7. Water absorption rates of the CPA-blended concrete for coated and uncoated specimens

Accepted / Not Edited

3.4.2 Capillary Water Absorption of CPA-blended concrete specimens with epoxy surface coatings at 28 and 56 days

Figures 8–9 present the sorptivity development and capillary suction behavior of incorporating CPA-blended concrete specimens with epoxy surface coatings at 28 and 56 days of curing. Water absorption due to capillary action was evaluated as a function of exposure time, while sorptivity coefficients were obtained from the linear relationship between the cumulative mass gain per unit area and the square root of time, in accordance with ASTM C1585.

At 28 days, the control mix exhibited the weakest linear relationship between cumulative absorption and the square root of time, with a correlation coefficient of $R^2 = 0.8252$ (Table 8), indicating non-uniform capillary absorption behavior associated with an immature pore structure. In contrast, CPA-modified specimens generally demonstrated stronger linearity, with correlation coefficients ranging from 0.8682 to 0.9800. The CPA-5 and CPA-20 mixtures showed the highest correlations ($R^2 = 0.9770$ and 0.9800, respectively), suggesting more stable and predictable absorption kinetics at early curing ages. The slightly lower correlation recorded for CPA-10 ($R^2 = 0.8682$) may be attributed to competing effects of pore refinement and internal porosity associated with CPA particle characteristics.

At 56 days, a notable improvement in sorptivity behavior was observed for all mixes, reflecting continued hydration and progressive densification of the cementitious matrix. The control mix exhibited a substantial increase in correlation coefficient ($R^2 = 0.9653$), indicating a more refined pore network at later ages. Similarly, CPA-modified mixes maintained high correlation coefficients, ranging between 0.8810 and 0.9751. The CPA-10 mixture recorded the highest value at this age ($R^2 = 0.9751$), confirming its superior capillary absorption stability and supporting its optimal performance observed in the mechanical properties assessment. Conversely, the CPA-20 mix showed a reduced correlation coefficient ($R^2 = 0.8810$), suggesting increased pore connectivity or heterogeneity at higher replacement levels.

Overall, the results indicate that CPA incorporation enhances the consistency of capillary absorption behavior compared to the control mixture, particularly at moderate replacement levels. While CPA-modified overlays exhibited slightly higher sorptivity than the control at early ages, this behavior is attributed to the inherent micro-, meso-, and macroporous structure of CPA particles, which influences moisture transport pathways. Nevertheless, the strong correlation coefficients observed at 56 days suggest that the synergistic effects of cement hydration, filler action, and nucleation provided by finely calcined CPA contribute to long-term pore refinement and improved durability performance. These findings are consistent with previous studies on agro-waste ash-modified HPCs, which emphasize the critical role of replacement level and particle size distribution in governing transport properties.

Accepted / Not Edited

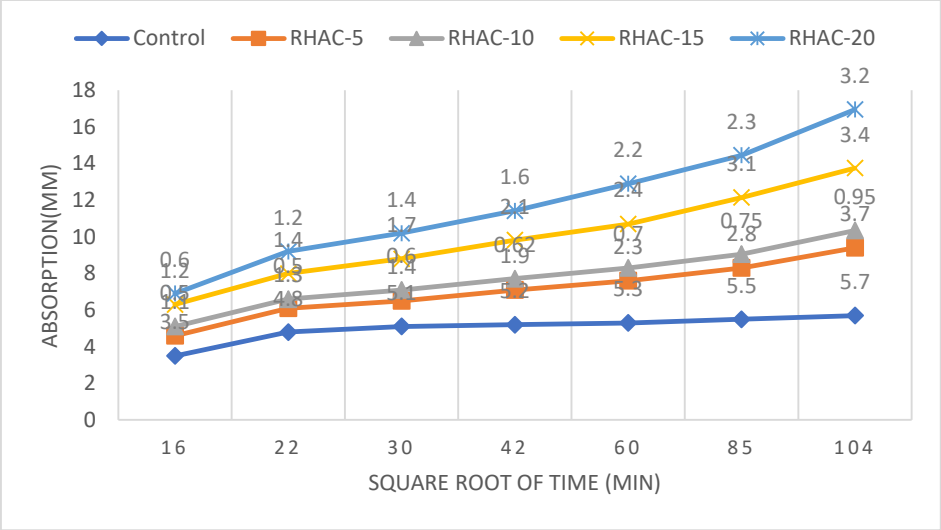


Fig. 8. Sorptivity characteristics of CPA-blended concrete specimens with epoxy surface coating at 28 days

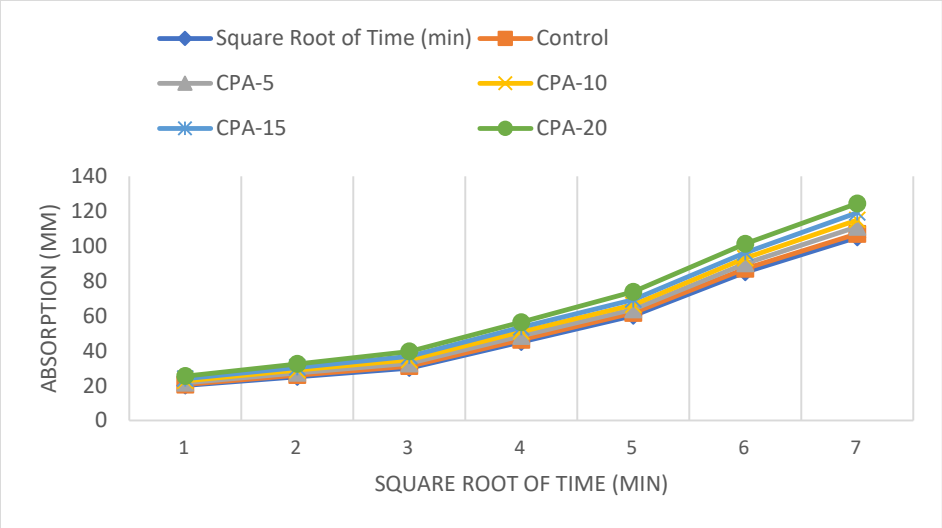


Fig. 9. Sorptivity characteristics of CPA-blended concrete with epoxy surface coating at 56 days

Table 8: Summary of Sorptivity Correlation Coefficients (R^2) of CPA--blended concrete specimens

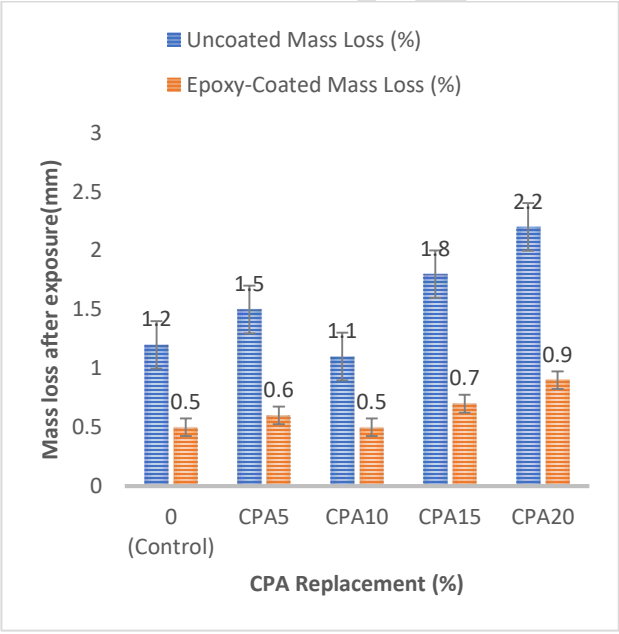
Mix ID	R^2 (28 Days)	R^2 (56 Days)
Control	0.8252	0.9653
CPA-5	0.9770	0.9602
CPA-10	0.8682	0.9751
CPA-15	0.9728	0.9521
CPA-20	0.9800	0.8810

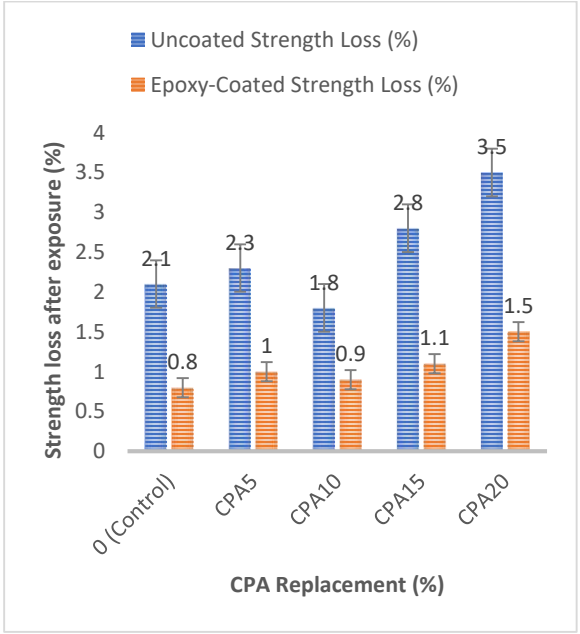
3.4.3 Sulphate and Acid Resistance

Figure 10 a&b presents the mass and compressive strength losses of uncoated and epoxy-coated CPA-blended concrete specimens after exposure to sulphate and acidic conditions at 56 days. In the case of uncoated specimens, both mass and strength losses progressively increased with higher CPA replacement levels. For instance, the 0% CPA control lost 1.2% of mass and 2.1% of compressive strength, whereas the 20% CPA specimen experienced 2.2% mass loss and 3.5% strength loss. This trend is attributed to increased porosity and reduced availability of calcium-bearing phases at higher CPA levels, which compromise the matrix's resistance to chemical attack.

Interestingly, the 10% CPA replacement level exhibited the lowest strength loss among the CPA-blended uncoated specimens (1.8%), suggesting an optimal balance between cement dilution and microstructural refinement. The secondary formation of calcium–silicate–hydrate (C–S–H) gel at this level likely improved pore structure and reduced the ingress of aggressive ions, enhancing chemical durability. This observation is consistent with previous studies showing that low- to moderate-level pozzolanic replacements can improve resistance to sulphate and acid attack via secondary C–S–H formation (Abdulmatin et al., 2023; W. Xu et al., 2016).

Epoxy-coated specimens consistently demonstrated significantly lower mass and strength losses across all CPA levels. For example, even the 20% CPA-coated sample experienced only 0.9% mass loss and 1.5% strength loss, highlighting the effectiveness of the coating in acting as a physical barrier to aggressive ions. The results underscore the synergistic benefit of combining moderate CPA replacement with epoxy surface protection to enhance chemical durability, consistent with prior research on surface coatings for cementitious materials in harsh environments (Abuzeid et al., 2024; Naderi & Rahbari, 2021).





ed / Not Edited

Fig. 10. (a) Mass loss of CPA-blended concrete after 56 days of exposure (b) Strength loss of CPA-blended concrete after 56 days of exposure.

3.4.4 Carbonation Resistance

Figure 11 shows the carbonation depth of uncoated and epoxy-coated CPA-blended concrete specimens at 56 days. For uncoated specimens, carbonation depth increased with higher CPA replacement levels, from 3.2 mm in the control to 4.7 mm at 20% CPA. This trend reflects the reduced availability of calcium hydroxide in CPA-blended concretes, which lowers the matrix's buffering capacity and facilitates deeper CO_2 ingress. These results are consistent with prior studies showing that increased pozzolanic replacement can increase carbonation susceptibility due to reduced free calcium hydroxide (Celik et al., 2019; Tang et al., 2022).

In contrast, epoxy-coated specimens exhibited a significant reduction in carbonation depth, exceeding 50% across all replacement levels. For example, the 20% CPA-coated specimen had a carbonation depth of 2.2 mm compared to 4.7 mm for its uncoated counterpart. Statistical analysis confirmed that these reductions were significant at the 95% confidence level ($p < 0.05$). The epoxy coating effectively limited CO_2 diffusion into the concrete, maintaining internal alkalinity and improving the protection of embedded reinforcement. Similar protective effects of surface coatings have been reported in previous research, emphasizing their role in mitigating carbonation-related deterioration in both conventional and blended concretes (GivKashi, 2025; Taffese et al., 2025).

Overall, these findings highlight that combining moderate CPA replacement with epoxy surface protection can simultaneously enhance sustainability and long-term durability, offering an effective strategy to control carbonation in cementitious materials.

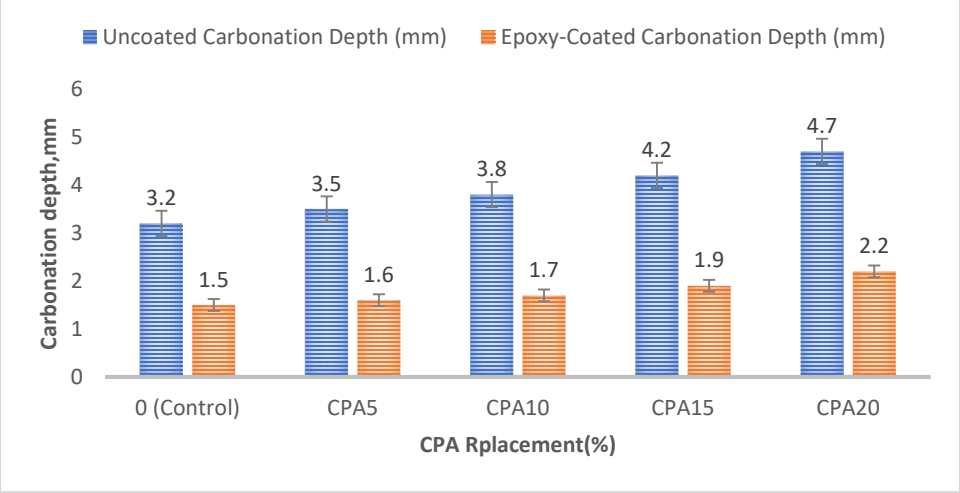


Fig. 11. Carbonation depth of uncoated and epoxy-coated CPA-blended concrete specimens at 56 days

3.4.5 Statistical Optimization of CPA Content

A multi-criteria optimization approach incorporating compressive strength, durability indicators, and strength retention under aggressive exposure conditions identified 10% CPA replacement as

the optimal dosage. At this level, the concrete exhibited delayed but favorable strength development, reduced sulphate-induced degradation, and acceptable carbonation resistance.

Furthermore, the incorporation of epoxy surface coating significantly expanded the viable replacement range, as even higher CPA contents demonstrated improved durability performance when external surface protection was applied. This indicates a synergistic interaction between internal microstructural refinement induced by pozzolanic reactions and external barrier protection provided by epoxy coating. Such synergy offers a robust pathway for maximizing sustainability while maintaining long-term performance in aggressive service environments.

Table 9 provides a consolidated comparison of the mechanical and durability performance of the control mix, CPA10 uncoated concrete, and CPA10 epoxy-coated concrete. While CPA10 without coating achieved comparable compressive strength to the control and improved chemical resistance, the application of epoxy coating resulted in substantial gains in strength retention, reduced transport properties, and more than 50% reduction in carbonation depth. This confirms that the optimal performance is achieved through the synergistic combination of 10% CPA replacement and surface epoxy protection.

Table 9. Summary comparison of mechanical and durability performance for Control, CPA10 uncoated, and CPA10 epoxy-coated concrete.

Performance Indicator	Control (0% CPA, Uncoated)	CPA10 Uncoated	CPA10 Epoxy-Coated
28-day compressive strength (MPa)	15.46 ± 0.42	15.20 ± 0.40	19.10 ± 0.48
Flexural strength at 28 days (MPa)	3.09	3.04	≈3.45–3.60
Water absorption at 56 h (%)	0.146	0.168	0.167
Sorptivity trend (56 days)	Moderate pore refinement	Improved vs. control	Lowest effective ingress
Correlation coefficient R^2 (56 days sorptivity)	0.9653	0.9751	>0.97
Mass loss after chemical exposure at 56 days (%)	1.2	≈1.0–1.1	≤0.5
Compressive strength loss after chemical exposure (%)	2.1	1.8 (lowest uncoated)	≈1.0–1.2
Carbonation depth at 56 days (mm)	3.2	~3.8	~1.6–1.8
Overall durability performance	Baseline	Improved internal densification	Best (internal + external protection)

5. Conclusions

This study investigated the combined use of CPA as a supplementary cementitious material and epoxy surface coating as an external protection system for improving the mechanical and durability performance of Portland limestone cement concrete exposed to aggressive environments. Based on the experimental findings, the following conclusions were drawn:

Accepted / Not Edited

1. CPA demonstrated promising pozzolanic characteristics. The controlled combustion of cassava peel produced an ash containing approximately 80 wt.% SiO_2 with a predominantly amorphous structure. The irregular and porous morphology of the ash suggests that CPA can contribute to both secondary pozzolanic reactions and particle-packing effects within the cementitious matrix, supporting its application as a low-calcium supplementary cementitious material.

2. The influence of CPA replacement was strongly dependent on the replacement level. Increasing CPA content generally reduced early-age strength, particularly at higher replacement levels, owing primarily to dilution and the slower development of pozzolanic reactions. Nevertheless, 10% CPA exhibited effective strength development, achieving a 28-day compressive strength of 15.20 MPa, which was comparable to the 15.46 MPa recorded for the control concrete. Replacement levels exceeding 15% resulted in a more pronounced reduction in the mechanical performance of the uncoated concrete.

3. Epoxy surface coating substantially improved strength retention and mechanical performance. The application of the epoxy coating enhanced the performance of CPA-containing concrete, with the CPA10-coated mixture attaining a 28-day compressive strength of 19.10 MPa compared with 15.20 MPa for the corresponding uncoated mixture, representing an increase of approximately 24%. Flexural strength also increased by more than 15%. These improvements indicate that the coating provided an effective external barrier and contributed to crack-bridging and confinement effects within the concrete surface region.

4. The combined CPA–epoxy system provided enhanced resistance to environmental deterioration. The incorporation of CPA contributed to matrix refinement, while the epoxy coating restricted the ingress of water and aggressive chemical species. The coated CPA10 concrete exhibited very low water absorption (approximately 0.17%), more than 40% lower chemically induced strength loss than the corresponding uncoated concrete, and a reduction of more than 50% in carbonation depth. These results demonstrate the complementary roles of internal matrix modification and external surface protection in mitigating deterioration.

5. The CPA10–epoxy system provided the most balanced performance among the mixtures investigated. The combination of 10% CPA replacement and epoxy surface protection offered a favourable balance between mechanical performance and resistance to water ingress, chemical attack, and carbonation. Rather than relying solely on increased cement content or high levels of supplementary cementitious material replacement, the results demonstrate the potential of combining moderate CPA incorporation with an external protective barrier to achieve enhanced durability.

6. The findings support the valorisation of cassava-processing residues in durable concrete applications. The use of CPA provides a pathway for converting an agricultural residue into

Accepted / Not Edited

a value-added supplementary cementitious material, while the epoxy coating provides additional protection where concrete is exposed to aggressive service conditions. The proposed dual-protection approach therefore has potential for applications requiring improved durability; however, further investigation under long-term field exposure, cyclic wetting–drying conditions, and broader chemical concentrations is required before large-scale structural application.

6. Availability of Data and Materials

Data will be made available on request from the corresponding author

7. Acknowlegement

This research received no external funding. The article processing charge (APC) was funded by the Tshwane University of Technology, Pretoria, South Africa.

8. Declaration

All respondents provided consent to participate in the research. Also, the authors confirm they have had no involvement with artificial intelligence (AI) tools in the writing of this article.

9. References

Abdulmatin, A., Khongpermgoson, P. S., Sanit-in, S., Jaturapitakkul, C., Tangchirapat, W., Khomwan, N., & Pham, T. M. (2023). Bottom ash as an alternative pozzolanic material to produce eco-friendly, high-quality chloride-resistant concrete. *Iranian Journal of Science and Technology, Transactions of Civil Engineering*, *47*(2), 829–842. https://doi.org/10.1007/s40996-022-00932-8.

Abuzeid, M. A., Bassuoni, M. T., & Sakr, M. R. (2024). Effect of Polymer/Nano-Clay Coatings on the Performance of Concrete with High-Content Supplementary Cementitious Materials under Harsh Exposures. *Materials*, *17*(5), 1030. https://doi.org/10.3390/ma17051030.

Adebisi, J. A., Agunsoye, J. O., Bello, S. A., Kolawole, F. O., Ramakokovhu, M. M., Daramola, M. O., & Hassan, S. B. (2019). Extraction of silica from sugarcane bagasse, cassava periderm and maize stalk: proximate analysis and physico-chemical properties of wastes. *Waste and Biomass Valorization*, *10*(3), 617–629.https://doi.org/10.1007/s12649-017-0089-5.

Astm, C. (2012). Standard test methods for chemical resistance of mortars, grouts, and monolithic surfacings and polymer concretes. *ASTM International*. https://doi.org/10.1520/C0267-01R12.

Carlsson, L. A., & Du, E. (2017). Water uptake in polymer composites with voids. In *Durability of Composites in a Marine Environment 2* (pp. 33–57). Springer. https://doi.org/10.1007/978-3-319-65145-3_3.

Celik, K., Hay, R., Hargis, C. W., & Moon, J. (2019). Effect of volcanic ash pozzolan or limestone replacement on hydration of Portland cement. *Construction and Building Materials*, *197*, 803–812. https://doi.org/10.1016/j.conbuildmat.2018.11.193.

Chung, D. D. L. (2018). *Multifunctional cement-based materials*. CRC Press. https://doi.org/10.1201/9781315273235.

Accepted / Not Edited

De La Rosa, A., Rena, C. Y., & Ruiz, G. (2025). An optimized procedure for cleaner concrete production with reduced CO2 emissions. *Case Studies in Construction Materials*, *23*, e05075. https://doi.org/10.1016/j.cscm.2025.e05075.

Elnaggar, E. M., Elsokkary, T. M., Shohide, M. A., El-Sabbagh, B. A., & Abdel-Gawwad, H. A. (2019). Surface protection of concrete by new protective coating. *Construction and Building Materials*, *220*, 245–252. https://doi.org/10.1016/j.conbuildmat.2019.06.026.

En, B. S. (2005). *Tests for mechanical and physical properties of aggregates—*. October. https://doi.org/10.3403/BSEN1097.

Gao, Y., Luo, J., Zhang, J., Ejaz, M. A., & Liu, L. (2025). Advances in Nano-Reinforced Polymer-Modified Cement Composites: Synergy, Mechanisms, and Properties. *Buildings*, *15*(15), 2598. https://doi.org/10.3390/buildings15152598.

GivKashi, M. R. (2025). Durability of 3D printed concrete containing air-entraining agent: evaluating the importance of carbonation resistance. *Engineering, Construction and Architectural Management*, 1–22. https://doi.org/10.1108/ECAM-06-2025-0939.

Iro, U. I., Alaneme, G. U., Attah, I. C., Ganasen, N., Duru, S. C., & Olaiya, B. C. (2024). Optimization of cassava peel ash concrete using central composite design method. *Scientific Reports*, *14*(1), 7901. https://doi.org/10.1038/s41598-024-58555-0.

Kewalramani, M., & Khartabil, A. (2021). Porosity evaluation of concrete containing supplementary cementitious materials for durability assessment through volume of permeable voids and water immersion conditions. *Buildings*, *11*(9), 378. https://doi.org/10.3390/buildings11090378.

Khushefati, W. H., Shihata, A., & Ahmed, E. A. (2025). Performance evaluation of green concrete incorporating Saudi natural pozzolana: State-of-the-Art. *Iranian Journal of Science and Technology, Transactions of Civil Engineering*, 1–32.https://doi.org/10.1007/s40996-025-02047-2.

Kim, S.-K., Jang, I.-Y., & Yang, H.-J. (2020). Strength development characteristics of concrete replaced with different waste glasses from display industry as a cementitious material. *KSCE Journal of Civil Engineering*, *24*(8), 2485–2494. https://doi.org/10.1007/s12205-020-0223-y.

Knight, K. A., Cunningham, P. R., & Miller, S. A. (2023). Optimizing supplementary cementitious material replacement to minimize the environmental impacts of concrete. *Cement and Concrete Composites*, *139*, 105049. https://doi.org/10.1016/j.cemconcomp.2023.105049.

Li, C., Tang, Z., Ju, J. W., & Zhong, J. (2025). Engineering Interfacial Transition Zone with Polymer/CNT Nanocomposites Coating: Break the Dilemma Between Strength and Damping. *Composites Part B: Engineering*, 112910. https://doi.org/10.1016/j.compositesb.2025.112910.

Liang, R., Liu, Q., Hou, D., Li, Z., & Sun, G. (2022). Flexural strength enhancement of cement paste through monomer incorporation and in situ bond formation. *Cement and Concrete Research*, *152*, 106675. https://doi.org/10.1016/j.cemconres.2021.106675.

Liu, Y., Wang, J., Hu, S., Cao, S., & Wang, F. (2022). Enhancing the mechanical behaviour of concretes through polymer modification of the aggregate-cement paste interface. *Journal of Building Engineering*, *54*, 104605.https://doi.org/10.1016/j.jobe.2022.104605.

Mandal, A., & Rajput, S. P. S. (2025). Advances in alkali-activation of ceramic waste-based pozzolana in concrete and mortar: a comprehensive review. *Waste and Biomass Valorization*, 1–22. https://doi.org/10.1007/s12649-025-02993-y.

Mishra, U. C., Sarsaiya, S., & Gupta, A. (2022). A systematic review on the impact of cement industries on the natural environment. *Environmental Science and Pollution Research*, *29*(13), 18440–18451. https://doi.org/10.1007/s11356-022-18672-7.

Mohammadi, A., & Ramezanianpour, A. M. (2023). Investigating the environmental and economic impacts of using

Accepted / Not Edited

supplementary cementitious materials (SCMs) using the life cycle approach. *Journal of Building Engineering*, *79*, 107934. https://doi.org/10.1016/j.jobe.2023.107934.

Naderi, M., & Rahbari, R. (2021). Efficiency of coating layers used for harsh environmental conditions protection of CFRP-strengthened concrete. *Journal of Building Engineering*, *44*, 102892. https://doi.org/10.1016/j.jobe.2021.102892.

Naseem, Z., Shamsaei, E., Sagoe-Crentsil, K., & Duan, W. (2023). Microstructural and polymer film interaction mechanisms: Insights of GO-reinforced polymer-modified cement composites. *Journal of Building Engineering*, *80*, 107962. https://doi.org/10.1016/j.jobe.2023.107962.

Nath, P. C., Ojha, A., Debnath, S., Sharma, M., Sridhar, K., Nayak, P. K., & Inbaraj, B. S. (2023). Biogeneration of valuable nanomaterials from agro-wastes: A comprehensive review. *Agronomy*, *13*(2), 561.https://doi.org/10.3390/agronomy13020561.

Nduka, D. O., Olawuyi, B. J., Fagbenle, O. I., & Fonteboa, B. G. (2022). Assessment of the durability dynamics of high-performance concrete blended with a fibrous rice husk ash. *Crystals*, *12*(1), 75.https://doi.org/10.3390/cryst12010075.

Ogbonna, C., Mbadike, E., & Alaneme, G. U. (2020). Characterisation and use of Cassava peel ash in concrete production. *Computational Engineering and Physical Modeling*, *3*(2), 12–28. https://doi.org/10.22115/CEPM.2020.223035.1091.

Ogunbode, E. B., Nyakuma, B. B., Jimoh, R. A., Lawal, T. A., & Nmadu, H. G. (2023). Mechanical and microstructure properties of cassava peel ash–based kenaf bio-fibrous concrete composites. *Biomass Conversion and Biorefinery*, *13*(8), 6515–6525. https://doi.org/10.1007/s13399-021-01588-6.

Onsongo, S. K., Olukuru, J., Munyao, O. M., & Mwabonje, O. (2025). The role of agricultural ashes (rice husk ash, coffee husk ash, sugarcane bagasse ash, palm oil fuel ash) in cement production for sustainable development in Africa. *Discover Sustainability*, *6*(1), 1–25. https://doi.org/10.1007/s43621-025-00841-6.

Prempeh, C. O., Formann, S., Schliermann, T., Dizaji, H. B., & Nelles, M. (2021). Extraction and characterization of biogenic silica obtained from selected agro-waste in Africa. *Applied Sciences*, *11*(21), 10363. https://doi.org/10.3390/app112110363.

Rajendran, S., Shanmugam, V., Sanjeevi, S., Yang, Y.-L., Marimuthu, U., Palani, G., Veerasimman, A., & Trilaksana, H. (2025). Prosopis juliflora biochar-based hybrid composites: Mechanical property assessment and development prospects. *Cleaner Engineering and Technology*, *26*, 100955. https://doi.org/10.1016/j.clet.2025.100955.

Ramakrishnan, T., Raja Karthikeyan, K., Tamilselvan, V., Sivakumar, S., Gangodkar, D., Radha, H. R., Narain Singh, A., & Asrat Waji, Y. (2022). Study of various epoxy-based surface coating techniques for anticorrosion properties. *Advances in Materials Science and Engineering*, *2022*(1), 5285919. https://doi.org/10.1155/2022/5285919.

Rao, P. V. C. (2020). Effects of matrix modification on mechanical and durability characteristics of polymer composites through variations in micro fillers, macro fillers and fibers. *Construction and Building Materials*, *235*, 117505.https://doi.org/10.1016/j.conbuildmat.2019.117505.

Sadowski, Ł., Kampa, Ł., Chowaniec, A., Królicka, A., Żak, A., Abdoulpour, H., & Vantadori, S. (2021). Enhanced adhesive performance of epoxy resin coating by a novel bonding agent. *Construction and Building Materials*, *301*, 124078. https://doi.org/10.1016/j.conbuildmat.2021.124078.

Samad, S., & Shah, A. (2017). Role of binary cement including Supplementary Cementitious Material (SCM), in production of environmentally sustainable concrete: A critical review. *International Journal of Sustainable Built Environment*, *6*(2), 663–674. https://doi.org/10.1016/j.ijsbe.2017.07.003.

Santhanam, K., Reshma, E. K., & George, C. (2025). Exploring the potential of alkali-activated cassava peel ash for early-age geopolymer concrete strength development. *Construction and Building Materials*, *498*, 144062.

Accepted / Not Edited

https://doi.org/10.1016/j.conbuildmat.2025.144062.

Sbahieh, S., McKay, G., Nurdiawati, A., & Al-Ghamdi, S. G. (2025). The sustainability of partial and total replacement of Ordinary Portland Cement: A deep dive into different concrete mixtures through life cycle assessment. *Journal of Building Engineering*, *108*, 112830. https://doi.org/10.1016/j.jobe.2025.112830.

British Standards Institution. (2009). Testing hardened concrete—Part 3: Compressive strength of test specimens (BS EN 12390-3:2009). https://doi.org/10.3403/30164906.

Taffese, W. Z., Hilloulin, B., Villagran Zaccardi, Y., Marani, A., Nehdi, M. L., Hanif, M. U., Kamath, M., Nunes, S., von Greve-Dierfeld, S., & Kanellopoulos, A. (2025). Machine learning in concrete durability: challenges and pathways identified by RILEM TC 315-DCS towards enhanced predictive models. *Materials and Structures*, *58*(4), 145. https://doi.org/10.1617/s11527-025-02664-3.

Tang, Y., Liu, G., Schollbach, K., Chen, Y., Chen, W., & Brouwers, H. J. H. (2022). Re-cementation effects by carbonation and the pozzolanic reaction on LWAs produced by hydrated cement paste powder. *Journal of Cleaner Production*, *377*, 134529. https://doi.org/10.1016/j.jclepro.2022.134529.

Xu, K., Yang, J., He, H., Wei, J., & Zhu, Y. (2025). Influences of Additives on the Rheological Properties of Cement Composites: A Review of Material Impacts. *Materials*, *18*(8), 1753. https://doi.org/10.3390/ma18081753.

Xu, W., Lo, T. Y., Wang, W., Ouyang, D., Wang, P., & Xing, F. (2016). Pozzolanic reactivity of silica fume and ground rice husk ash as reactive silica in a cementitious system: A comparative study. *Materials*, *9*(3), 146. https://doi.org/10.3390/ma9030146.

Zhang, M., Xu, H., Zeze, A. L. P., Liu, X., & Tao, M. (2022). Coating performance, durability and anti-corrosion mechanism of organic modified geopolymer composite for marine concrete protection. *Cement and Concrete Composites*, *129*, 104495.https://doi.org/10.1016/j.cemconcomp.2022.104495.

Zhang, X., Du, M., Fang, H., Shi, M., Zhang, C., & Wang, F. (2021). Polymer-modified cement mortars: Their enhanced properties, applications, prospects, and challenges. *Construction and Building Materials*, *299*, 124290.https://doi.org/10.1016/j.conbuildmat.2021.124290.

Zhao, Z., Qu, X., & Li, J. (2020). Application of polymer modified cementitious coatings (PCCs) for impermeability enhancement of concrete. *Construction and Building Materials*, *249*, 118769. https://doi.org/10.1016/j.conbuildmat.2020.118769.

Zhutovsky, S., & Hooton, R. D. (2019). Role of sample conditioning in water absorption tests. *Construction and Building Materials*, *215*, 918–924. https://doi.org/10.1016/j.conbuildmat.2019.04.249.

Accepted / Not Edited